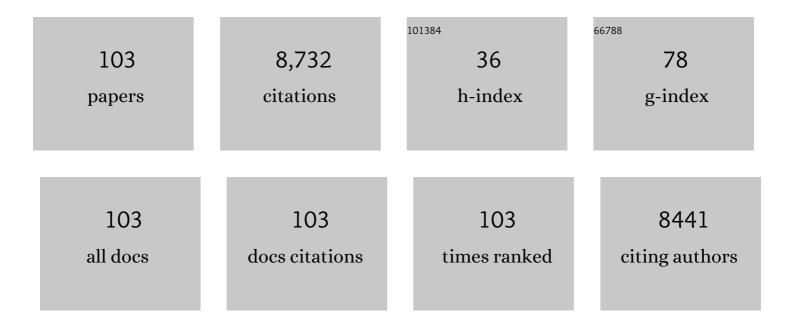
## Zachary C Holman

List of Publications by Year in descending order

Source: https://exaly.com/author-pdf/2727183/publications.pdf Version: 2024-02-01



#	Article	IF	CITATIONS
1	23.6%-efficient monolithic perovskite/silicon tandem solar cells with improved stability. Nature Energy, 2017, 2, .	19.8	1,204
2	High-efficiency Silicon Heterojunction Solar Cells: A Review. Green, 2012, 2, 7-24.	0.4	725
3	Resolving spatial and energetic distributions of trap states in metal halide perovskite solar cells. Science, 2020, 367, 1352-1358.	6.0	699
4	Triple-halide wide–band gap perovskites with suppressed phase segregation for efficient tandems. Science, 2020, 367, 1097-1104.	6.0	669
5	Current Losses at the Front of Silicon Heterojunction Solar Cells. IEEE Journal of Photovoltaics, 2012, 2, 7-15.	1.5	479
6	Hybrid Solar Cells from P3HT and Silicon Nanocrystals. Nano Letters, 2009, 9, 449-452.	4.5	379
7	Grain Engineering for Perovskite/Silicon Monolithic Tandem Solar Cells with Efficiency of 25.4%. Joule, 2019, 3, 177-190.	11.7	329
8	Overcoming Redox Reactions at Perovskite-Nickel Oxide Interfaces to Boost Voltages in Perovskite Solar Cells. Joule, 2020, 4, 1759-1775.	11.7	284
9	Infrared light management in high-efficiency silicon heterojunction and rear-passivated solar cells. Journal of Applied Physics, 2013, 113, .	1.1	270
10	Efficient Semitransparent Perovskite Solar Cells for 23.0%â€Efficiency Perovskite/Silicon Fourâ€Terminal Tandem Cells. Advanced Energy Materials, 2016, 6, 1601128.	10.2	240
11	Selecting tandem partners for silicon solar cells. Nature Energy, 2016, 1, .	19.8	229
12	Minimizing Current and Voltage Losses to Reach 25% Efficient Monolithic Two-Terminal Perovskite–Silicon Tandem Solar Cells. ACS Energy Letters, 2018, 3, 2173-2180.	8.8	194
13	>21% Efficient Silicon Heterojunction Solar Cells on n- and p-Type Wafers Compared. IEEE Journal of Photovoltaics, 2013, 3, 83-89.	1.5	187
14	Simplified interconnection structure based on C60/SnO2-x for all-perovskite tandem solar cells. Nature Energy, 2020, 5, 657-665.	19.8	186
15	Nature-inspired chiral metasurfaces for circular polarization detection and full-Stokes polarimetric measurements. Light: Science and Applications, 2019, 8, 78.	7.7	184
16	Monocrystalline CdTe solar cells with open-circuit voltage over 1 V and efficiency of 17%. Nature Energy, 2016, 1, .	19.8	172
17	Controlling Thin-Film Stress and Wrinkling during Perovskite Film Formation. ACS Energy Letters, 2018, 3, 1225-1232.	8.8	148
18	Improving metal reflectors by suppressing surface plasmon polaritons: a priori calculation of the internal reflectance of a solar cell Light: Science and Applications, 2013, 2, e106-e106	7.7	143

#	Article	IF	CITATIONS
19	Optimization of Si NC/P3HT Hybrid Solar Cells. Advanced Functional Materials, 2010, 20, 2157-2164.	7.8	125
20	Germanium and Silicon Nanocrystal Thin-Film Field-Effect Transistors from Solution. Nano Letters, 2010, 10, 2661-2666.	4.5	119
21	Defect engineering in wide-bandgap perovskites for efficient perovskite–silicon tandem solar cells. Nature Photonics, 2022, 16, 588-594.	15.6	112
22	Optical modeling of wide-bandgap perovskite and perovskite/silicon tandem solar cells using complex refractive indices for arbitrary-bandgap perovskite absorbers. Optics Express, 2018, 26, 27441.	1.7	102
23	Record Infrared Internal Quantum Efficiency in Silicon Heterojunction Solar Cells With Dielectric/Metal Rear Reflectors. IEEE Journal of Photovoltaics, 2013, 3, 1243-1249.	1.5	92
24	Techno-economic viability of silicon-based tandem photovoltaic modules in the United States. Nature Energy, 2018, 3, 747-753.	19.8	86
25	Parasitic absorption in the rear reflector of a silicon solar cell: Simulation and measurement of the sub-bandgap reflectance for common dielectric/metal reflectors. Solar Energy Materials and Solar Cells, 2014, 120, 426-430.	3.0	75
26	An All-Gas-Phase Approach for the Fabrication of Silicon Nanocrystal Light-Emitting Devices. Nano Letters, 2012, 12, 2822-2825.	4.5	66
27	Series Resistance Measurements of Perovskite Solar Cells Using <i>J<sub>sc</sub></i> 〓 <i>V<sub>oc</sub></i> Measurements. Solar Rrl, 2019, 3, 1800378.	3.1	61
28	PVMirror: A New Concept for Tandem Solar Cells and Hybrid Solar Converters. IEEE Journal of Photovoltaics, 2015, 5, 1791-1799.	1.5	57
29	Amorphous silicon carbide passivating layers for crystalline-silicon-based heterojunction solar cells. Journal of Applied Physics, 2015, 118, .	1.1	56
30	Analysis of lateral transport through the inversion layer in amorphous silicon/crystalline silicon heterojunction solar cells. Journal of Applied Physics, 2013, 114, 074504.	1.1	54
31	Passivation, conductivity, and selectivity in solar cell contacts: Concepts and simulations based on a unified partial-resistances framework. Journal of Applied Physics, 2019, 126, .	1.1	49
32	Nanocrystal Inks without Ligands: Stable Colloids of Bare Germanium Nanocrystals. Nano Letters, 2011, 11, 2133-2136.	4.5	44
33	Manufacturing 100-µm-thick silicon solar cells with efficiencies greater than 20% in a pilot production line. Physica Status Solidi (A) Applications and Materials Science, 2015, 212, 13-24.	0.8	44
34	15.3%-Efficient GaAsP Solar Cells on GaP/Si Templates. ACS Energy Letters, 2017, 2, 1911-1918.	8.8	44
35	Accuracy of expressions for the fill factor of a solar cell in terms of open-circuit voltage and ideality factor. Journal of Applied Physics, 2016, 120, .	1.1	41
36	Solution-Processed Germanium Nanocrystal Thin Films as Materials for Low-Cost Optical and Electronic Devices. Langmuir, 2009, 25, 11883-11889.	1.6	36

#	Article	IF	CITATIONS
37	Current-Matched III–V/Si Epitaxial Tandem Solar Cells with 25.0% Efficiency. Cell Reports Physical Science, 2020, 1, 100208.	2.8	36
38	Understanding what limits the voltage of polycrystalline CdSeTe solar cells. Nature Energy, 2022, 7, 400-408.	19.8	36
39	Silicon heterojunction solar cells with effectively transparent front contacts. Sustainable Energy and Fuels, 2017, 1, 593-598.	2.5	34
40	Contact Resistivity of the p-Type Amorphous Silicon Hole Contact in Silicon Heterojunction Solar Cells. IEEE Journal of Photovoltaics, 2020, 10, 54-62.	1.5	34
41	20%-efficient epitaxial GaAsP/Si tandem solar cells. Solar Energy Materials and Solar Cells, 2019, 202, 110144.	3.0	33
42	Reducing sputter induced stress and damage for efficient perovskite/silicon tandem solar cells. Journal of Materials Chemistry A, 2022, 10, 1343-1349.	5.2	27
43	CdCl2 passivation of polycrystalline CdMgTe and CdZnTe absorbers for tandem photovoltaic cells. Journal of Applied Physics, 2018, 123, .	1.1	26
44	Aerosol Impaction-Driven Assembly System for the Production of Uniform Nanoparticle Thin Films with Independently Tunable Thickness and Porosity. ACS Applied Nano Materials, 2018, 1, 4351-4357.	2.4	26
45	Photonic Crystal Waveguides for >90% Light Trapping Efficiency in Luminescent Solar Concentrators. ACS Photonics, 2020, 7, 2122-2131.	3.2	26
46	Preâ€Fabrication Gettering and Hydrogenation Treatments for Silicon Heterojunction Solar Cells: A Possible Path to >700 mV Openâ€Circuit Voltages Using Lowâ€Lifetime Commercialâ€Grade pâ€Type Czochralski Silicon. Solar Rrl, 2018, 2, 1700221.	3.1	25
47	Plasma synthesis of group IV quantum dots for luminescence and photovoltaic applications. Pure and Applied Chemistry, 2008, 80, 1901-1908.	0.9	24
48	Sub-micrometer random-pyramid texturing of silicon solar wafers with excellent surface passivation and low reflectance. Solar Energy Materials and Solar Cells, 2020, 218, 110761.	3.0	24
49	Loss Analysis of Monocrystalline CdTe Solar Cells With 20% Active-Area Efficiency. IEEE Journal of Photovoltaics, 2017, 7, 900-905.	1.5	23
50	Ultra-wide-bandgap AlGaN homojunction tunnel diodes with negative differential resistance. Applied Physics Letters, 2019, 115, .	1.5	23
51	Plasma-initiated rehydrogenation of amorphous silicon to increase the temperature processing window of silicon heterojunction solar cells. Applied Physics Letters, 2016, 109, .	1.5	22
52	Absolute absorption cross sections of ligand-free colloidal germanium nanocrystals. Applied Physics Letters, 2012, 100, .	1.5	21
53	Visualizing light trapping within textured silicon solar cells. Journal of Applied Physics, 2020, 127, .	1.1	19
54	Defect engineering of pâ€type silicon heterojunction solar cells fabricated using commercialâ€grade lowâ€lifetime silicon wafers. Progress in Photovoltaics: Research and Applications. 2021, 29, 1165-1179	4.4	16

#	Article	IF	CITATIONS
55	Progress with Defect Engineering in Silicon Heterojunction Solar Cells. Physica Status Solidi - Rapid Research Letters, 2021, 15, 2100170.	1.2	16
56	Carrier scattering mechanisms limiting mobility in hydrogen-doped indium oxide. Journal of Applied Physics, 2018, 123, .	1.1	15
57	Origins of hydrogen that passivates bulk defects in silicon heterojunction solar cells. Applied Physics Letters, 2019, 115, .	1.5	15
58	Hetero-emitter GaP/Si solar cells with high Si bulk lifetime. , 2016, , .		14
59	Complete regeneration of BO-related defects in n-type upgraded metallurgical-grade Czochralski-grown silicon heterojunction solar cells. Applied Physics Letters, 2018, 113, .	1.5	14
60	Understanding Transport in Hole Contacts of Silicon Heterojunction Solar Cells by Simulating TLM Structures. IEEE Journal of Photovoltaics, 2020, 10, 363-371.	1.5	13
61	Investigation of the Selectivity of Carrier Transport Layers in Wideâ€Bandgap Perovskite Solar Cells. Solar Rrl, 2021, 5, 2100107.	3.1	13
62	Robust passivation of CdSeTe based solar cells using reactively sputtered magnesium zinc oxide. Solar Energy Materials and Solar Cells, 2021, 233, 111388.	3.0	13
63	Lowâ€refractiveâ€index nanoparticle interlayers to reduce parasitic absorption in metallic rear reflectors of solar cells. Physica Status Solidi (A) Applications and Materials Science, 2017, 214, 1700179.	0.8	12
64	Silicon wafers with optically specular surfaces formed by chemical polishing. Journal of Materials Science: Materials in Electronics, 2016, 27, 10270-10275.	1.1	10
65	Self-Aligned Selective Area Front Contacts on <i>Poly</i> -Si/SiO <i> <sub>x</sub> </i> Passivating Contact <i>c</i> -Si Solar Cells. IEEE Journal of Photovoltaics, 2022, 12, 678-689.	1.5	10
66	Evaluation of metal oxides prepared by reactive sputtering as carrier-selective contacts for crystalline silicon solar cells. , 2015, , .		9
67	Monocrystalline CdTe/MgCdTe Double-Heterostructure Solar Cells With ZnTe Hole Contacts. IEEE Journal of Photovoltaics, 2017, 7, 307-312.	1.5	9
68	Monocrystalline 1.7-eV-Bandgap MgCdTe Solar Cell With 11.2% Efficiency. IEEE Journal of Photovoltaics, 2018, 8, 581-586.	1.5	9
69	GaAs/silicon PVMirror tandem photovoltaic miniâ€module with 29.6% efficiency with respect to the outdoor global irradiance. Progress in Photovoltaics: Research and Applications, 2019, 27, 469-475.	4.4	9
70	Pâ€ŧype Upgraded Metallurgicalâ€Grade Multicrystalline Silicon Heterojunction Solar Cells with Openâ€Circuit Voltages over 690 mV. Physica Status Solidi (A) Applications and Materials Science, 2019, 216, 1900319.	0.8	9
71	CdTe nBn photodetectors with ZnTe barrier layer grown on InSb substrates. Applied Physics Letters, 2016, 109, .	1.5	8
72	Substrateâ€independent analysis of microcrystalline silicon thin films using UV Raman spectroscopy. Physica Status Solidi (B): Basic Research, 2017, 254, 1700204.	0.7	8

#	Article	IF	CITATIONS
73	PVMirrors: Hybrid PV/CSP collectors that enable lower LCOEs. AIP Conference Proceedings, 2017, , .	0.3	8
74	Scanning Laser-Beam-Induced Current Measurements of Lateral Transport Near-Junction Defects in Silicon Heterojunction Solar Cells. IEEE Journal of Photovoltaics, 2014, 4, 154-159.	1.5	7
75	Aluminum–silicon interdiffusion in silicon heterojunction solar cells with a-Si:H(i)/a-Si:H(n/p)/Al rear contacts. Journal Physics D: Applied Physics, 2021, 54, 134002.	1.3	7
76	Silicon Nitride Barrier Layers Mitigate Minority-Carrier Lifetime Degradation in Silicon Wafers During Simulated MBE Growth of III–V Layers. IEEE Journal of Photovoltaics, 2019, 9, 431-436.	1.5	6
77	< 700 mV Open-Circuit Voltages on Defect-Engineered P-type Silicon Heterojunction Solar Cells on Czochralski and Multicrystalline Wafers. , 2018, , .		5
78	Thermal model to quantify the impact of sub-bandgap reflectance on operating temperature of fielded PV modules. Solar Energy, 2021, 220, 246-250.	2.9	5
79	Aerosol impaction-driven assembly produces evenly dispersed nanoparticle coating on polymeric water treatment membranes. Journal of Nanoparticle Research, 2020, 22, 1.	0.8	4
80	Evaluating the Impact of and Solutions to Light-induced Degradation in Silicon Heterojunction Solar Cells. , 2019, , .		3
81	1.7 eV MgCdTe double-heterostructure solar cells for tandem device applications. , 2016, , .		2
82	19.5%-Efficient Back-Contact Silicon Heterojunction Solar Cell With Self Aligned Metallization Using Multilayer Aluminum Foils. , 2018, , .		2
83	Numerical analysis of bifacial silicon-based tandem devices: Shifts in the optimum top-cell bandgap with varying albedo. , 2018, , .		2
84	Understanding Transport in Heterojunction Contact Stacks by Simulating Silicon Heterojunction TLM Structures. , 2018, , .		2
85	Inserting a Low-Refractive-Index Dielectric Rear Reflector into PERC Cells: Challenges and Opportunities. , 2019, , .		2
86	Sputtered Aluminum Oxide and p <sup>+</sup> Amorphous Silicon Back-Contact for Improved Hole Extraction in Polycrystalline CdSe <sub>x</sub> Te <sub>1-x</sub> and CdTe Photovoltaics. , 2019, , .		2
87	Power Losses in the Front Transparent Conductive Oxide Layer of Silicon Heterojunction Solar Cells: Design Guide for Single-Junction and Four-Terminal Tandem Applications. IEEE Journal of Photovoltaics, 2020, 10, 326-334.	1.5	2
88	Sub-bandgap features in CdSeTe solar cells: Parsing the roles of material properties and cell optics. , 2021, , .		2
89	Amorphous silicon carbide high contrast gratings as highly efficient spectrally selective visible reflectors. Optics Express, 2022, 30, 26787.	1.7	2
90	Properties of hydrogenated indium oxide prepared by reactive sputtering with hydrogen gas. , 2016, , .		1

6

#	Article	IF	CITATIONS
91	P-type Hybrid Heterojunction Solar Cells Naturally Incorporating Gettering and Bulk Hydrogenation. , 2018, , .		1
92	Impact of Tabula Rasa and Phosphorus Diffusion Gettering on 21% Heterojunction Solar Cells Based on n-Type Czochralski-Grown Upgrade Metallurgical-Grade Silicon. , 2018, , .		1
93	Assessing TiOx as a hole-selective contact for silicon heterojunction solar cells. , 2021, , .		1
94	Amorphous silicon/crystalline silicon heterojunction solar cells — Analysis of lateral conduction through the inversion layer. , 2014, , .		0
95	Crystalline silicon passivation with amorphous silicon carbide layers. , 2016, , .		Ο
96	Properties and Imaging of Thick Doped Amorphous Silicon in Direct Contact with Aluminum For Use in Silicon Heterojunction Solar Cells. , 2018, , .		0
97	Co-Sublimated Polycrystalline Cd <inf>1-x</inf> Zn <inf>x</inf> Te Films for Multi-junction Solar Cells. , 2018, , .		Ο
98	AC-STEM and HRSEM Investigation of Silica Nanoparticle Film Structure. Microscopy and Microanalysis, 2019, 25, 2008-2009.	0.2	0
99	Elevating Low-Quality Silicon Wafers For High-Efficiency Silicon Heterojunction Solar Cell Applications. , 2019, , .		0
100	Photoluminescence Study of the MgxZn1-xO/CdSeyTe1-y Interface: The Effect of Oxide Bandgap and Resulting Band Alignment. , 2021, , .		0
101	Manufacturable Perovskite/Silicon Tandems with Solution-Processed Perovskites on Textured Silicon Bottom Cells. , 2020, , .		0
102	Diffusion profiles beneath silicon heterojunction contacts reduce contact resistivity and increase efficiency. , 2020, , .		0
103	Determination of Series Resistance in CdSeTe/CdTe Solar Cells by the Jsc–Voc Method. , 2020, , .		0